






# TreeSpecies-PC2DT: Automated Tree Species Modeling from Point Clouds to Digital Twins

Like Gobeawan<sup>1</sup>, Xuan Liu<sup>1</sup>, Chi Wan Lim<sup>1</sup>, Venugopalan Raghavan<sup>1</sup>, Joyjit Chatteraj<sup>1</sup>,  
Jan Schindler<sup>2</sup> and Feng Yang<sup>1</sup>

<sup>1</sup>*Institute of High Performance Computing, Agency for Science, Technology and Research,  
1 Fusionopolis Way #16-16 Connexis, Singapore, Singapore*

<sup>2</sup>*Manaaki Whenua - Landcare Research, Wellington, New Zealand*

*schindlerj@landcareresearch.co.nz*

**Keywords:** Digital Twin, Tree Species Model, Point Cloud Data, Tree Branch Reconstruction, Procedural Modeling, Optimisation.

**Abstract:** 3D digital twin trees for a city-scale have been limited to low-resolution, static shape models due to challenges in automation/scalability, cost performance, tree growth dynamics, species complexities and compatibilities with simulations and virtual city platforms. To address those challenges for high-resolution tree models, we propose an automated workflow of generating large-scale, lightweight, dynamic digital-twin tree species models from point cloud data. Species digital twins are modelled as detailed hierarchical branch structures by solving for all species profile parameters through stages of branch reconstruction from point cloud data, species profiling by machine learning, tropism transfer, optimisation and species growth modelling based on botany and limited field survey. We show that the generated high-resolution tree models can be lightweight while representing their true species characteristics and dynamic botanical architecture (branching patterns and growth processes).


## 1 INTRODUCTION


### 1.1 Motivation


With the rise of artificial intelligence (AI) technologies for automation tasks, the digital twin (DT) for objects, processes or systems in real life are gaining traction in manufacturing, aviation and transportation, healthcare, medicine (Barricelli et al., 2019), and more slowly, smart city domain and city-scale DT for urban planning, sustainability and climate change mitigation (Mylonas et al., 2021). DT cities poses many challenges in coverage and operationalisation (Lei et al., 2023) due to complexities in urban life comprising physical structures and living things (human beings, greeneries and animals). In particular, DT cities often focus on physical structures at various


levels of details and leave out the dynamic structure of greeneries that play essential social-economic, environmental roles in green cities such as Singapore (National Research Foundation, 2018). More specifically, DT trees for a city-scale have been limited to low-resolution/simplistic, static watertight shape models for their cost performance and compatibilities with simulations.


On the other hand, addressing dynamic species-level trees and their interactions with the environments in the form of high-resolution species digital twins will enable more comprehensive simulations and analysis, leading to better insights and improved urban planning. However, this poses a grand challenge in automating and maintaining the modelling of millions of dynamically growing tree species at a large/city scale based on remote sensing data. Firstly, remote sensing data, such as (lower-resolution) satellite imagery and (higher-resolution) LiDAR (light detection and ranging) scanned point cloud, generally contain fuzzy information of tree characteristics due to noises, obstacles and other limitations in their acquisition. Thus, they require manual pre-processing

<sup>a</sup>  <https://orcid.org/0000-0001-6501-6394>

<sup>b</sup>  <https://orcid.org/0000-0002-1760-9993>

<sup>c</sup>  <https://orcid.org/0000-0002-8319-9742>

<sup>d</sup>  <https://orcid.org/0000-0003-0831-4218>

<sup>e</sup>  <https://orcid.org/0000-0003-1910-8954>

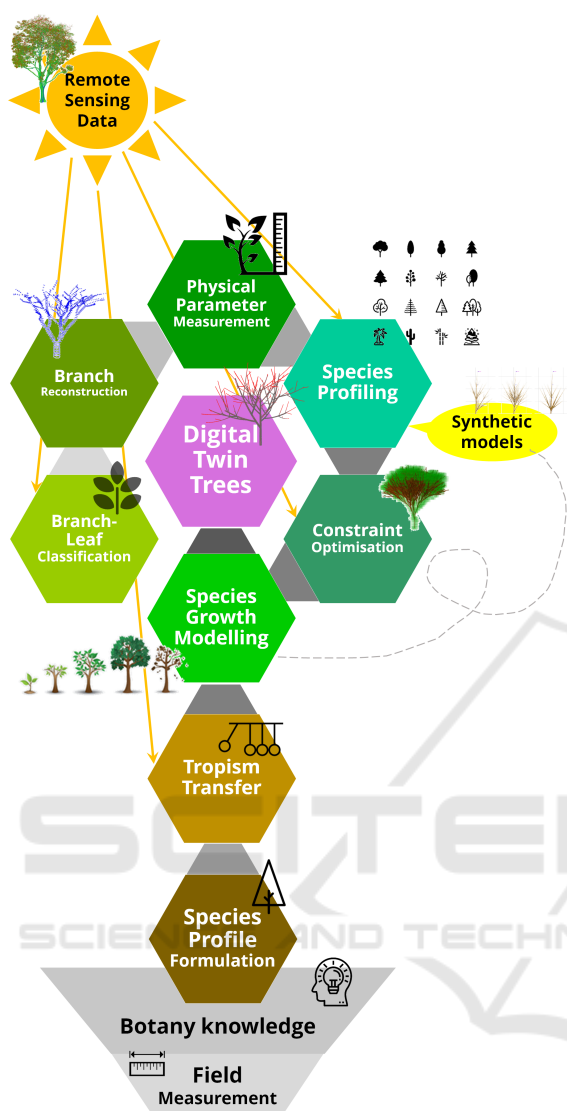


Figure 1: Automated digital twin tree species model from remote sensing data.

and patching in order to produce estimated models with limited accuracies on the actual branch structure of the tree species. Secondly, temporal data of tree growths are very scarce. They can only be reliably inferred from high-resolution MLS (mobile laser scanning) point cloud or photogrammetry, whose acquisition is, in contrast, low in frequency (typically annually or biennially) for a city-wide campaign. Thirdly, such high-resolution data of millions of trees have an extremely low cost performance - they take considerable resources to exist dynamically on DT city platforms.

## 1.2 Problem Statements

This work seeks to automatically generate city-scale, lightweight and dynamic tree models to represent the trees at a high-resolution species level, i.e. displaying high-fidelity branch patterns and growth processes of individual trees. To remain lightweight, the species models should not be represented by mesh surfaces or volumes with high count of polygons or voxels.

## 1.3 Literature Review

Most DT city tools seek to model (in 3D) static physical structures at various level of details, yet stop short in modelling greeneries as low-resolution, static 3D shape tree models (Lin et al., 2018) in virtual cities (National Research Foundation, 2018; Government, 2019). For high-resolution trees, (Gobeawan et al., 2018; Stava et al., 2014; Makowski et al., 2019) attempted to generate dynamic tree models from remote sensing data to high-resolution textured polygon models, however they are not validated for a city-scale implementation as their high polygon counts lead to tendency to overload the platform rendering in real time.

In the field of FSPM (functional-structural plant modelling), there are many works (Godin and Sinoquet, 2005; Vos et al., 2010; Sievänen et al., 2014; Yi et al., 2018; Talle and Kosinka, 2020; Niese et al., 2020) on modelling individual tree species along with their growth and functions at high levels of detail, yet very specific to certain individual or species, hence they are not scalable. At the core of FSPM, L-system (Prusinkiewicz and Lindenmayer, 1996) is a good candidate to produce lightweight species models, as it adopts a procedural modelling approach of using a small set of rules to generate a wide variety of tree models. However, there have been very few concerted efforts to establish a procedural-based framework for DT species at the city-scale.

As such, we propose an automated workflow of city-scale, dynamic tree species modelling from remote sensing data to digital twin tree models.

## 2 METHODOLOGY

Our automated workflow, herein codenamed as TreeSpecies-PC2DT, starts with the point cloud data of a tree as an input and generates a final output of a digital twin species model (Figure 1). The workflow comprises of 5 main modules:

- branch segmentation and reconstruction for tree measurements

- species profiling
- tropism transfer
- constraint optimisation
- species growth modelling

Each digital twin tree is individually modelled to closely match the actual trees by a set of parameters with different values that define their unique species profiles. The values of these parameters are derived for an individual tree by reconstructing preliminary branch structures from point cloud data by branch point classification and branch/skeleton reconstruction. Due to fuzziness in the crown where leaves might obstruct high-order branches (twigs), the branch reconstruction stage is only effective in measuring trunk and branch components which are not concealed by leaves and other objects within the tree crown. Hence, the tree measurements can be obtained for trunk parameters such as trunk height and diameter, trunk pitch and roll angles, as well as first order branch count and first branching pitch and roll angles.

Subsequently, the ML (machine learning)-based species profiling module will use the reconstructed branches to predict values of other unknown tree parameters with a certain level of confidence. The ML is trained to recognise or estimate tree parameter values by learning from the big data of synthetic species models which were generated based on true botanic growth and branching processes incorporated in the species growth modelling module. The knowledge learnt is then transferred to train on reconstructed branches derived from the scarce real point cloud data.

Along with the former two modules above, the tropism transfer module estimates the tree tropism, i.e. the growth response of the tree to environment stimuli. The tropism transfer uses the reconstructed branch structure and existing tropism models in literature to derive the change in growth direction along the tree stem and the stem elasticity parameter of the tree along its proximal (trunk) and distal (branches).

Finally, the remaining unknown parameter values (or parameter values with low confidence) will be solved by the optimisation module. The completely solved parameter configuration will be fed into the species growth modelling module to generate the digital twin species models.

The species growth modelling module contains a set of growth rules that dictate how the tree grows over time. The growth rules are formulated from botany knowledge and limited field survey/measurements.

As a whole workflow, TreeSpecies-PC2DT is able to automatically process city-scale individual

trees from the point cloud data into the botanically-representative, lightweight, and dynamic digital twin species models.

## 2.1 Input Data

The input to TreeSpecies-PC2DT workflow is LiDAR (light detection and ranging) point clouds with resolutions ranging from high to low. The point cloud resolution depends on the means of scanning, such as MLS (mobile laser scanning), TLS (terrestrial laser scanning), and ULS (UAV (unmanned aerial vehicle) laser scanning) or ALS (aerial laser scanning).

The main input data used for the workflow demonstration in this paper is the high-resolution MLS point cloud, which were acquired by Singapore Land Authority (SLA) (Soon and Khoo, 2017) using Riegl VMX-450 with a density of 40 points/m<sup>2</sup>. Individual tree point clouds were extracted using tree segmentation algorithms (Gobeawan et al., 2018). A group of MLS datasets are also placed on a plot (Figure 2) for testing the tree modelling workflow.



Figure 2: Individual MLS trees on a plot.

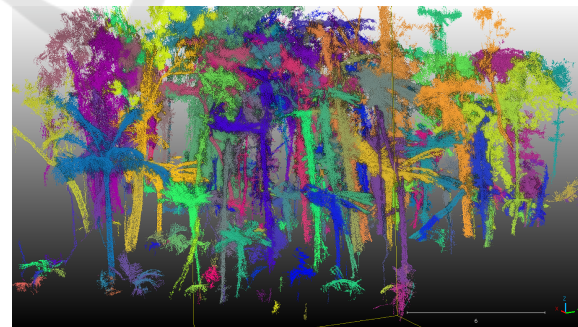


Figure 3: Segmented individual trees from subcanopy TLS data.

We also experimented with the subcanopy TLS data of a complex natural forest plot in New Zealand (Figure 3). The point cloud data was captured with a FARO Focus3D X 330 laser scanner in the Orongorongo Valley in the Greater Wellington Region, New Zealand. The study site is particularly challeng-

ing because of dense undergrowth including vines, a mixture of native species and rough terrain making accurate high-resolution measurements difficult. The point cloud was stitched together from several measurements with the help of survey reflectors placed in the field, and further post-processed for noise filtering, ground-vegetation classification, as well as woody material and stem segmentation and individual stems using point clustering. Starting at seeded stem locations, the entire individual trees were segmented using a region-growing algorithm.

## 2.2 Branch Segmentation and Reconstruction for Tree Measurements

This section entails branch segmentation (i.e. branch-leaf classification) and branch reconstruction for deriving tree measurements. While there have been works in tree measurements from point cloud data such as (Hartley et al., 2022), in general they still require labourious onsite survey to obtain measurements for higher order branches of the trees. Hence, we focus on automated tree measurements for lower order trunk and branches.

Given the input point cloud data of an individual tree, we perform branch-leaf classification to extract the tree’s woody points and then branch reconstruction to connect those woody points into a skeleton structure of branch centre points with their corresponding radii (Figure 4).

The branch segmentation and reconstruction algorithms are based on (Lim et al., 2020), producing an MTG (multiscale tree graph) detailing the hierarchical branch points with their radius and connectivity. Each node in the MTG file consists of a radius parameter to indicate the thickness of the branch. The first node of the MTG node is the tree base on the ground. Using the branch connectivity and radius values, we can derive values of an initial set of parameters for tree measurements, such as trunk height, trunk pitch and roll angles, trunk diameter and girth, branch pitch and roll angles, and number of first order branches (Figure 5). To get appropriate measurements, it is important to modify the MTG in (Lim et al., 2020) to consider the actual sizes of trunk and branches in determining the hierarchy of all nodes (stems and twigs), i.e. parent-child relationships at all branching points.

To do this, radii of all nodes corresponding to each branching point are compared, starting from the ground level of the trunk, i.e. the first node of the MTG. If any trunk node has a single child node, that child node is also assigned as the trunk node. In the

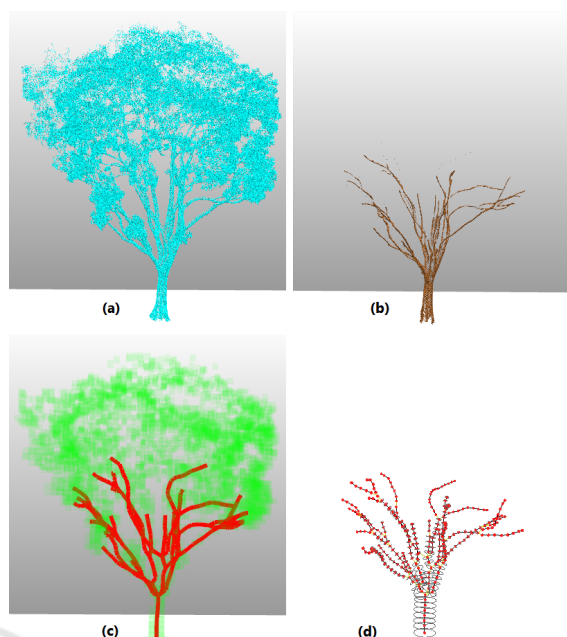


Figure 4: (a) Original point cloud, (b) woody point cloud, (c) reconstructed branch skeleton (red) superimposed with growth space (green), (d) hierarchy of branch centre points and their radii (MTG format).



Figure 5: Tree measurement diagram.

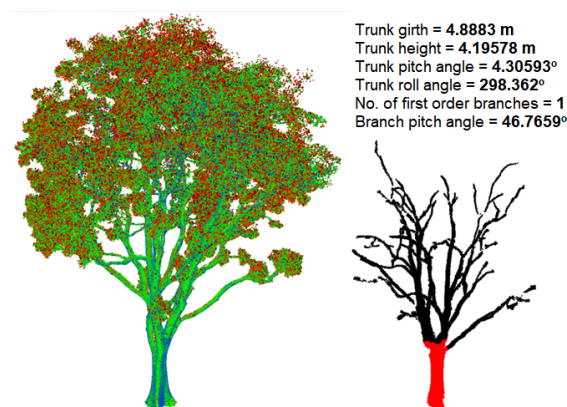


Figure 6: Woody segmentation and branch reconstruction for tree measurement of *Khaya senegalensis*.

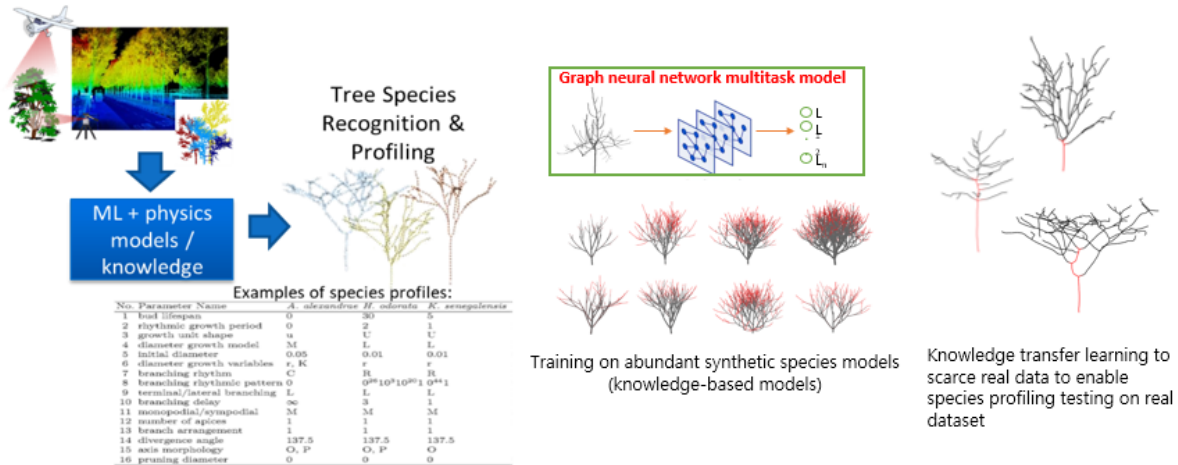


Figure 7: Species profiling flow.

case of a branching point with multiple child nodes, a simple test is applied to determine if any of the child node is a trunk node too. If the combined cross-sectional area of the child nodes is larger than the cross sectional area of the parent node, then the child with the largest radius assigned as the continuation of the trunk node.

Once all the trunk nodes are assigned, tree measurements can be derived (Figure 6). The trunk height can be computed by adding up the distances between adjacent trunk nodes. The trunk ground girth is taken as the circumference of the trunk node closest to the ground level. The trunk pitch angle is taken as the smallest angle from the up vector to the trunk axis, while the trunk roll angle is measured counter-clockwise from the North vector to the projected trunk axis on the horizontal plane. The number of first order branching is taken as the first instance of multiple child node encountered from ground up. The branch pitch and roll angles are derived from the first order branches with respect to the trunk.

### 2.3 Species Profiling

The species profiling module aims to determine the values of all species profile parameters with corresponding levels of confidence (Figure 7). If unknown parameters can be solved with an acceptable level of confidence, they are considered solved and subsequently passed to the next stage in the TreeSpecies-PC2DT workflow.

The species profiling work has been described in detail in (Chattoraj et al., 2022). In this work, ML-based method of knowledge transfer learning from abundant synthetic species data with known parameter values to scarce real tree data was devised to de-

tect species profile parameter values of a given real tree input.

The species profile parameters and their values (listed in Table 2) are collated from all runs and organised into XML (extensible markup language)-formatted:

- individual profiles for individual trees with their known individual and species information
- species profiles for known species with their species-specific statistics obtained from botany knowledge and field surveys, then bootstrapped by newly detected values from species profiling of incoming real tree data, and
- species library as a collection of species profiles and individual profiles.

The species library are used by the species growth modelling module (Section 2.6) to generate synthetic species data for training the species profiling module (Gobeawan et al., 2023).

### 2.4 Tropism Transfer

The tropism transfer module seeks to detect tropism characteristics (such as bending curvature and elasticity of tree trunk and branches) from reconstructed tree branches and to transfer the tropism onto DT species models. As tropism detection requires temporal data such as tree growth snapshots which are generally not present in individual reconstructed trees, we rely on growth snapshots of synthetic trees or experimental tropism data to derive ranges of values of relevant tropism parameters in our species growth modelling (Section 2.6).

While our preliminary work (Raghavan et al., 2023) performs a direct transfer of the trunk bend-

ing appearance from a tree point cloud skeleton to an individual tree model, the tropism transfer module in this paper expands it as a mapping of the trunk/branch bending appearance of a tree point cloud skeleton to a tropism model that predicts growth changes of a tree model in response to environment/external stimuli.

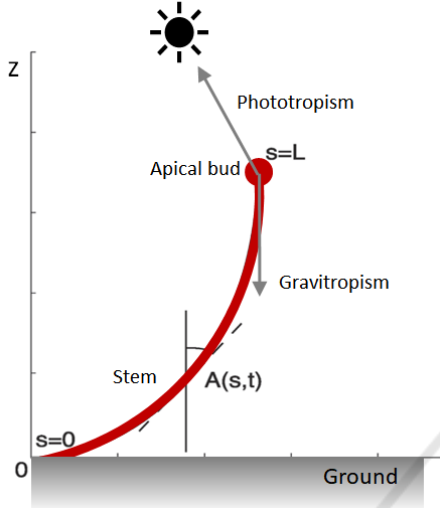


Figure 8: Diagram of phototropism and gravitropism on a stem.

Modelling of tropism, particularly the tree growth response to light (phototropism) and gravity (gravitropism) as well as its own ability to grow straight in the absence of environment stimuli (autotropism), has been done by deriving a mathematical representation of the behaviour of plants (Bastien et al., 2015; Moulton et al., 2020). In (Bastien et al., 2015), the tropism is modelled as changes in angles and curvatures of the part of the plant that is growing (Figure 8). Depending on the considered tropisms (phototropism, gravitropism and/or autotropism), angles and curvatures are linked to one or more tropism sensitivity parameters (photosensitivity, gravisensitivity and/or propriosensitivity) by partial differential equations (PDEs).

Our current work considers all three tropisms by adopting the  $A_R^C$  model in (Bastien et al., 2015) (Figure 8), which is formulated as

$$\frac{\partial C(s,t)}{\partial t} = -v(A(L,t)) - A_P - \beta A(s,t) - \gamma C(s,t) \quad (1)$$

where  $s$  represents the curvilinear coordinate of a node along a stem ( $s = 0$  at stem end at ground and  $s = L$  at the apical end),  $A(s,t)$  is the node's bending angle (with respect to up vector) at  $s$  and at time  $t$ ,  $C(s,t)$  is the local curvature at  $s$  and  $t$ ,  $A_P$  is the direction angle of light from down vector, while  $v$ ,  $\beta$  and  $\gamma$  are the photo-, gravi- and proprio- sensitivity coefficients

respectively.

As  $\frac{\partial A}{\partial s} = C$ , Equation 1 is complex to solve analytically, hence a numerical approach is adopted. While numerical approaches are capable of handling integro-differential equations, Equation 2 is assumed to ensure a better understanding of the underlying phenomena.

$$A(s,t) = A(0,t) + C(s,t)s \quad (2)$$

Thus, Equation 1 becomes

$$\frac{C_i^{k+1} - C_i^k}{\Delta t} = -v(A_i^k - A_P) - \beta A_i^k - \gamma C_i^k \quad (3)$$

where superscript  $k$  indicates the current time step while the subscript  $i$  indicates the current point along the growing member.

To solve Equation 3, we adopted an explicit time-stepping with a restriction on the value of  $\Delta t$  that can be used. Our tests indicate that the time-step  $\Delta t$  should range from  $1e^{-3}$  to  $1e^{-4}$  time units to ensure convergences for the angle and curvature values.

Assuming that the values of the tropism sensitivity parameters,  $v$ ,  $\beta$  and  $\gamma$  are obtained from available growth data (either from field experiments or analytics from synthetic tree data), the angles and curvatures of all points along the stem for each time step can be computed.

By solving all the tropism parameters above, we can generate species models with the same tropism behaviour of a tree input (Figure 9). Based on the inherent characteristics of each species, the exhibited tropism effect will be different even with the same specified values for the tropism parameters (refer to species profile parameters for tropism in Table 2).

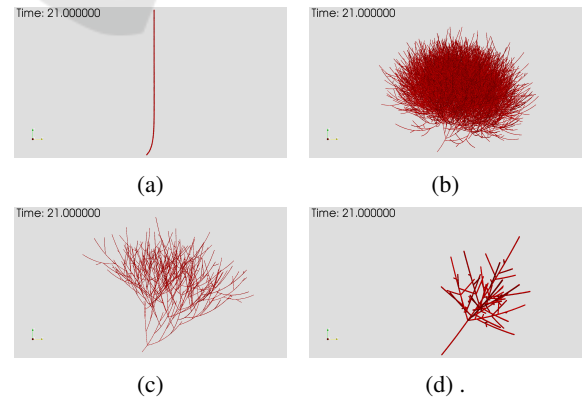


Figure 9: A tropism is transferred to four tree species: (a) *Archontophoenix alexandrae*, (b) *Khaya senegalensis*, (c) *Samanea saman*, (d) *Hopea odorata*.

Table 1: Optimised parameters for various tree samples.

Parameters	<i>Hopea odorata</i>	<i>Swietenia macrophylla</i>	<i>Khaya senegalensis</i>	<i>Tabebuia rosea</i>	<i>Sterculia parviflora</i>	<i>Syzygium grande</i>
Trunk pitch angle*, roll angle*	2.68, 248.48	3.68, 189.28	4.31, 298.36	0.57, 289.82	6.44, 305.45	13.39, 333.67
Trunk height*	1.65	3.68	4.2	5.18	2.41	3.27
Number of 1 <sup>st</sup> order branches*	2	4	1	2	2	3
Branch pitch angle*	60.89	32.54	46.77	42.68	38.94	45.90
Phyllotaxis: type <sup>#</sup>	2	1	1	2	1	1
Phyllotaxis: divergence angle <sup>#</sup>	90	137.5	137.5	90	137.5	137.5
Monopodial/sympodial branching <sup>#</sup>	Sympodial	Monopodial	Monopodial	Sympodial	Monopodial	Monopodial
Age	5	34	44	11	11	17
Branch roll angle	245.74	296.93	14.92	249.57	124.16	52.97
Diameter growth rate	0.014	0.76	0.94	0.39	0.55	0.51
Number of new nodes per bud	34	11	49	15	36	22
Internode length	0.05	0.03	0.03	0.09	0.05	0.04
Bud lifespan	0	0	6	0	3	0
Rhythmic growth period	1	0	6	5	0	0
Branching delay	0	1	7	2	5	2
Error (cost function)	11.6%	0.5%	3.0%	21.5%	18.0%	1.5%

\*parameters solved after branch reconstruction

<sup>#</sup>parameters solved after species profiling

## 2.5 Optimisation

The final round of solving for remaining parameters with unknown values or low confidences from branch reconstruction and species profiling modules is done by optimisation. The optimisation module utilises a genetic algorithm (GA) method to find the best configuration of species profile parameters within specified physical constraints (Gobeawan et al., 2021; Lim et al., 2023). An initial database is generated from a population of possible parameter configuration solutions over ranges of possible values appended with cost function evaluated for each solution. The algorithm then pairs a selection of the best solutions with a number of random solutions from the database, creating parent solutions. A successive generation of 4 child solutions are generated from the parent solution by making slight adjustments to their values. These successive generations along with their corresponding cost function elevations, are appended to update the database. This process continues iteratively until a predefined number of generations is reached or the cost meets the specified threshold.

The cost function of the optimisation measures a linear weighted distances between the solution and the physical constraints. These physical constraints include both macroscopic shape (i.e. crown shape and dimension) and microscopic structure of the target tree (i.e. trunk bending, measurements, growth space). Specifically, the growth space refers to a set of voxels within a uniform grid in the 3D

space derived from input point cloud data. Details of the cost function are described in (Gobeawan et al., 2021).

Table 1 shows the optimised parameters for individual trees of various species. It has 3 categories of parameters: (1) solved by branch reconstruction: trunk pitch angle, trunk roll angle, trunk height, number of first order branches and branch pitch angle, (2) solved by species profiling: phyllotaxis and monopodial/sympodial branching and (3) solved by optimisation: the rest of all parameters. Any solved parameters with low confidence levels in the previous modules (branch reconstruction and species profiling) will be re-solved by optimisation.

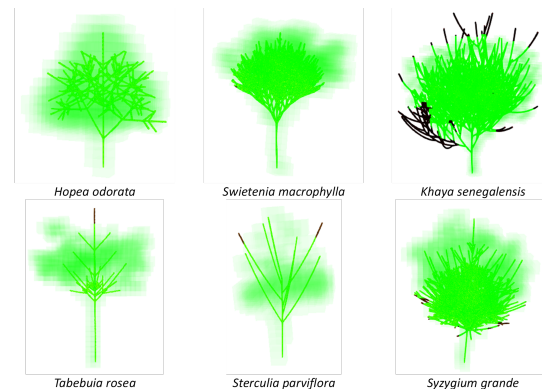


Figure 10: Optimised species models (black) within growth spaces (green).

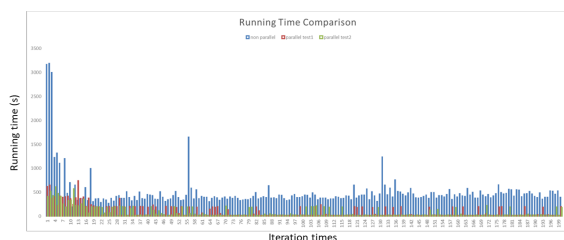


Figure 11: Comparison of running times for each iteration with and without parallelisation.

In addition, if the tree comes with identified species, the optimisation search space can be further reduced to within smaller ranges of parameter values specific to that species.

The optimisation process is set to terminate by a limited period of time or when the error  $E$  falls below 10%, whichever is earlier. Their corresponding tree models with given growth space (voxel spacing of 50cm, minimum of 5 points per voxel) are shown in Figure 10.

The optimisation process is also highly parallelised for improving system efficiency and running time. Figure 11 shows that the running time decreases linearly with the increase in the number of computing processors used.

## 2.6 Species Growth Modelling

The species growth modelling module aims to generate dynamically growing DT species models (Figure 12) based on the input values of species profile parameters. The mechanism and formulation of growth rules in this module is described in details in (Gobeawan et al., 2021). Further updates to the list of species profile parameters are shown in Table 2 to include tropism parameters. Additional growth parameters can be added to the list in order to simulate more phenomena and interactions between trees and environments.

In addition, synthetic models can be generated by varying the values of species profile parameters.

## 3 RESULTS AND DISCUSSION

We tested high-resolution MLS data of Singapore trees and low-resolution TLS data of New Zealand trees, both individually and as a scene of trees, in the TreeSpecies-PC2DT workflow.

Given an individual tree of known species *Khaya senegalensis* from MLS input data, the TreeSpecies-PC2DT workflow generates a DT species model with a good fit with the actual scanned tree (Figure 13).

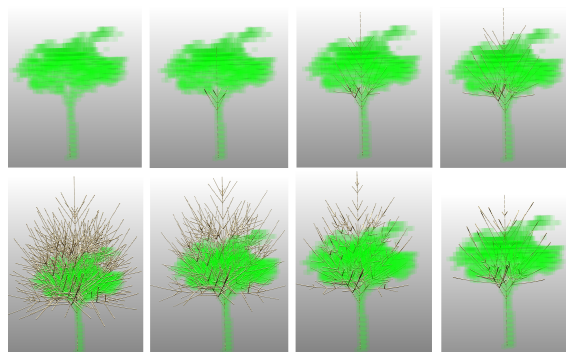


Figure 12: Clockwise from top left: Growth snapshots of a typical tree of species *Tabebuia rosea* grows from 1 to 17 years old, with a growth space reference (green) at 11 years old.

For an individual tree of unknown species from low-resolution TLS input data, the workflow generates a very simple DT model correspondingly, while capturing the essential bending and architecture of the input tree (Figure 14).

While time benchmark was not done in this experiment, we show the planting of DT species models in a plot for both MLS and TLS data in Figures 15 and 16 and observed stark difference in loading time for DT models (in seconds) and original point clouds (in minutes) on the same computer system. This shows the potential of lightweight DT species models for large-scale city platforms.

## 4 CONCLUSIONS

The proposed high-resolution, species-level representation DT models in MTG format is very lightweight yet representing fundamental species characteristics of branching patterns and dynamic growth, making them suitable for large scale simulations. While their visual appearance as not as realistic as high-polygon-count trees with textures, the DT species models correspond to the actual tree branch structure in reality. Meshing such DT species models as in (Lim et al., 2020) potentially turns the DT models into simulation-ready models - enabling many environmental simulations and analysis without using expensive high-resolution tree models.

Future works for TreeSpecies-PC2DT are planned for testing with more types of LiDAR data while evaluating the performance of DT species on virtual cities, in addition to expansion to include root of the trees in order to allow wider environment simulations using whole trees for tree health and safety management purposes.



Table 2: Species profile parameters.

No.	Parameter Name	Format	Unit	Description
<b>A</b>	<b><i>Growth process</i></b>			
1	bud lifespan	$\geq 0$	year	Lifespan of a bud, 0 if indeterminate
2	rhythmic growth period	$\geq 0$	year	Period of rhythmic growth to produce 1 GU, zero if continuous growth
3	growth unit shape	a choice	-	Unspecified (U), acrotonic (A), mesotonic (M), or basitonic (B)
4	diameter growth model	a choice	-	Relative growth rate (RGR): linear (L), exponential (E), power law (P), monomolecular (M), 3-param logistic (3PL), 4-param logistic (4PL), Gombertz (G)
5	initial diameter	$> 0$	meter	Non-zero minimum branch diameter
6	diameter growth variables $r, \beta, K, L$	ranges	t:day, M:cm,	Variables for RGR equation with respect to growth model
<b>B</b>	<b><i>Branching process</i></b>			
7	branching rhythm	a choice	-	Continuous (C), rhythmic (R), or diffuse (D)
8	rhythmic branching pattern	xxx	-	Binary rhythmic branching pattern of 0s and 1s
9	terminal/lateral branching	a choice	-	New branches are formed by lateral buds (L) or apical split (T)
10	branching delay	$\geq 0$	year	New branches grow out immediately (0) or after some delay
11	monopodial/sympodial branching	a choice	-	Apical stem remains dominant with emergence of lateral branches (M) or stops growing with emergence of dominant lateral branches (S)
12	no. of dominant apices	$\geq 1$	-	Sole or multiple dominant apices (scaffolds)
13	phyllotaxis type	a choice	-	Alternate (1), opposite (2), or whorled (n)
14	divergence angle	$0 \leq \theta \leq 180$	degree	Angle between two branches from adjacent rows
<b>C</b>	<b><i>Tropism</i></b>			One or multiple entries
15	tropism type	a choice	-	Gravitropism, phototropism, or autotropism
16	proximal response	a choice	-	Trunk responds towards/against stimulus, orthotropically/plagiotropically
17	distal response	a choice	-	Branches respond towards/against stimulus, orthotropically/plagiotropically
18	plagiotropic angle	a range, $0 \leq \theta < 90$	degree	For plagiotropy, at an angle from stimulus
19	elasticity	a range, $0 < E < 1$	-	Ease to bend
20	source format	a vector	-	Field, point, plane, or volume to respond to
21	pruning diameter	$\geq 0$	meter	To prune branches smaller than pruning diameter
<b>E</b>	<b><i>Constraints</i></b>			
22	growth space	a volume	-	Physical space occupied by the tree
23	age	a range, $\geq 1$	year	Simulation age for the species
24	trunk ground girth	a range, $> 0$	m	Circumference of trunk closest to ground level
25	trunk pitch angle	a range, $0 \leq \theta \leq 180$	degree	Angle between up vector and trunk axis closest to ground
26	trunk roll angle	a range, $0 \leq \theta < 360$	degree	Counter-clockwise (CCW) angle from North to trunk on ground
27	trunk height	a range, $\geq 0$	meter	Distance from ground to first branching point
28	no. of 1 <sup>st</sup> order branches	a range, $\geq 0$	-	At first branching point from bottom
29	branch pitch angle	a range, $0 \leq \theta \leq 180$	degree	From parent's head down to start of branch
30	branch roll angle	a range, $0 \leq \theta < 360$	degree	Rotate CCW around parent's head
31	diameter growth rate	a range, $0 \leq g \leq 1$	-	Normalised growth rate; first three decimals are mapped to diameter growth variables
32	number of new nodes	a range, $> 0$	/year	Number of nodes a bud produces in a year
33	internode length	a range, $\geq 0$	meter	Length of a segment between adjacent nodes

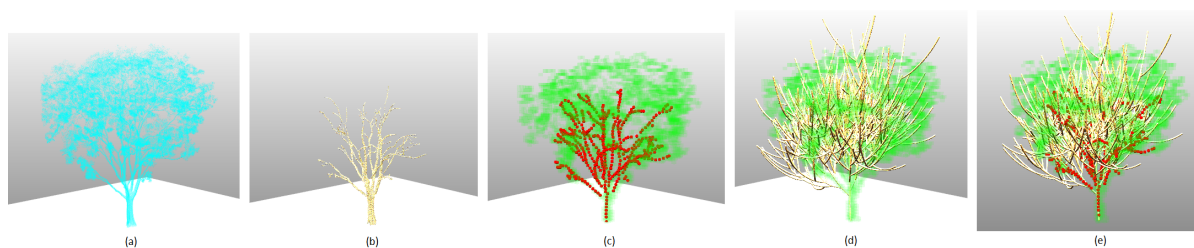


Figure 13: Generating DT species of *Khaya senegalensis* from MLS data: (a) MLS point cloud, (b) segmented branch point cloud, (c) reconstructed branch (red) within growth space (green), (d) DT species (yellow) within growth space (green), (e) DT species (yellow) superimposed with reconstructed branch (red) within growth space (green).

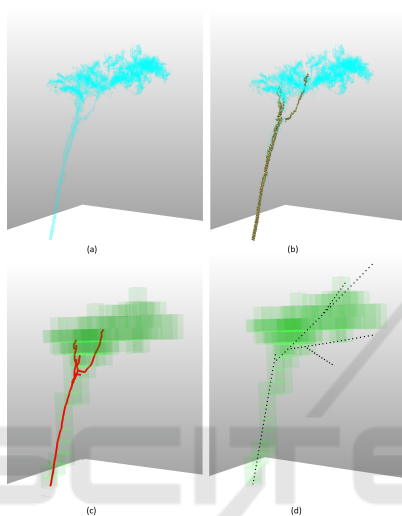


Figure 14: Generating a DT tree of unidentified species from TLS data: (a) TLS point cloud, (b) segmented branch point cloud (brown), (c) reconstructed branch (red) within growth space (green), (d) DT tree (black) within growth space (green).

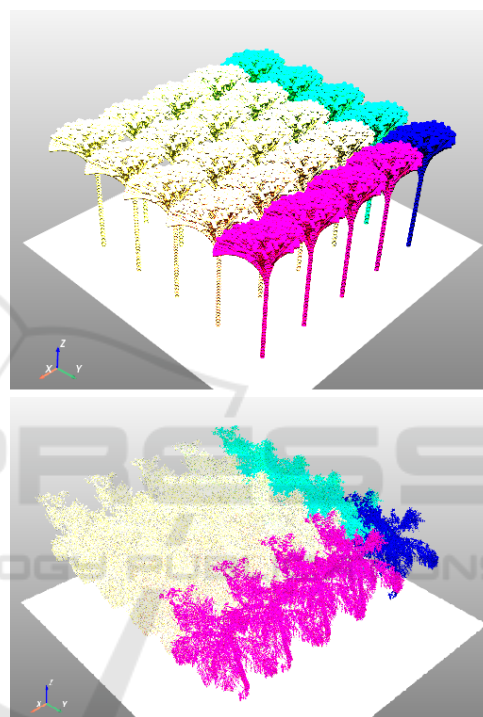


Figure 16: Comparison of a scene of lightweight DT palms (left) with a scene of denser TLS point clouds of palms (right).

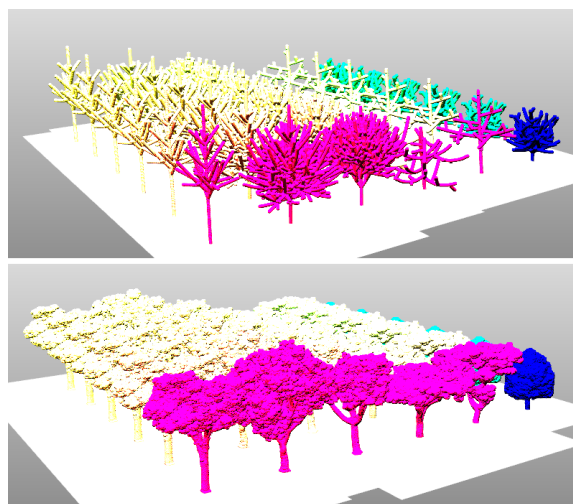


Figure 15: Comparison of a scene of lightweight DT species (top) with a scene of much denser MLS point clouds of the same tree species (bottom).

## ACKNOWLEDGEMENTS

This research/project is supported by the Catalyst: Strategic Fund from Government Funding, administered by the Ministry of Business Innovation & Employment, New Zealand under contract C09X1923, as well as the National Research Foundation, Singapore under its Industry Alignment Fund – Pre-positioning (IAF-PP) Funding Initiative. Any opinions, findings and conclusions or recommendations expressed in this material are those of the author(s) and do not reflect the views of National Research Foundation, Singapore.

## REFERENCES

- Barricelli, B. R., Casiraghi, E., and Fogli, D. (2019). A survey on digital twin: Definitions, characteristics, applications, and design implications. *IEEE Access*, 7:167653–167671.
- Bastien, R., Douady, S., and Mouliat, B. (2015). A unified model of shoot tropism in plants: Photo-, gravi- and proprioception. *PLoS computational biology*, 11:e1004037.
- Chattoraj, J., Yang, F., Lim, C. W., Gobeawan, L., Liu, X., and Raghavan, V. S. (2022). Knowledge-driven transfer learning for tree species recognition. In *2022 17th International Conference on Control, Automation, Robotics and Vision (ICARCV)*, pages 149–154.
- Gobeawan, L., Chattoraj, J., Yang, F., Lim, C. W., Liu, X., and Raghavan, V. S. G. (2023). Knowledge-based learning for plant phenotyping. In Chen, T.-W., Kahlen, A. F. K., and Stützel, H., editors, *10th International Conference on Functional-Structural Plant Models (FSPM2023)*, pages 140–141.
- Gobeawan, L., Lin, E. S., Tandon, A., Yee, A. T. K., Khoo, V. H. S., Teo, S. N., Su, Y., Lim, C. W., Wong, S. T., Wise, D. J., Cheng, P., Liew, S. C., Huang, X., Li, Q. H., Teo, L. S., Fekete, G. S., and Poto, M. T. (2018). Modeling trees for Virtual Singapore: From data acquisition to CityGML models. *International Archives of the Photogrammetry, Remote Sensing and Spatial Information Sciences*, XLII-4/W10:55–62.
- Gobeawan, L., Wise, D. J., Wong, S. T., Yee, A. T. K., Lim, C. W., and Su, Y. (2021). Tree species modelling for digital twin cities. *Transactions on Computational Science XXXVIII*, pages 17–35.
- Godin, C. and Sinoquet, H. (2005). Functional-structural plant modelling. *New Phytologist*, 166(3):705–708.
- Government, N. S. W. (2019). Nsw spatial digital twin.
- Hartley, R. J. L., Jayathunga, S., Massam, P. D., De Silva, D., Estarija, H. J., Davidson, S. J., Wuraola, A., and Pearce, G. D. (2022). Assessing the potential of backpack-mounted mobile laser scanning systems for tree phenotyping. *Remote Sensing*, 14(14).
- Lei, B., Janssen, P., Stoter, J., and Biljecki, F. (2023). Challenges of urban digital twins: A systematic review and a delphi expert survey. *Automation in Construction*, 147:104716.
- Lim, C. W., Gobeawan, L., Wong, S. T., Wise, D. J., Cheng, P., Poh, H. J., and Su, Y. (2020). Generation of tree surface mesh models from point clouds using skin surfaces. In *15th International Conference on Computer Graphics Theory and Applications*, pages 83–92.
- Lim, C. W., Liu, X., Gobeawan, L., Raghavan, V. S. G., Chattoraj, J., and Yang, F. (2023). Species model parameterisation. In Chen, T.-W., Kahlen, A. F. K., and Stützel, H., editors, *10th International Conference on Functional-Structural Plant Models (FSPM2023)*, pages 68–69.
- Lin, E.-S., Teo, L.-S., Yee, A.-T.-K., and Li, Q.-H. (2018). Populating large scale virtual city models with 3D trees. In *55th IFLA World Congress*, Singapore.
- Makowski, M., Hädrich, T., Scheffczyk, J., Michels, D. L., Pirk, S., and Paubicki, W. (2019). Synthetic silviculture: Multi-scale modeling of plant ecosystems. *ACM Trans. Graph.*, 38(4).
- Moulton, D., Oliveri, H., and Goriely, A. (2020). Multiscale integration of environmental stimuli in plant tropism produces complex behaviors. *Proceedings of the National Academy of Sciences (PNAS)*, 117:32226–32237.
- Mylonas, G., Kalogeras, A., Kalogeras, G., Anagnostopoulos, C., Alexakos, C., and Muñoz, L. (2021). Digital twins from smart manufacturing to smart cities: A survey. *IEEE Access*, 9:143222–143249.
- National Research Foundation (2018). Virtual Singapore. NRF website <https://www.nrf.gov.sg/programmes/virtual-singapore>.
- Niese, T., Pirk, S., Albrecht, M., Benes, B., and Deussen, O. (2020). Procedural urban forestry.
- Prusinkiewicz, P. and Lindenmayer, A. (1996). *The Algorithmic Beauty of Plants*. Springer-Verlag, Berlin, Heidelberg.
- Raghavan, V. S. G., Gobeawan, L., Lim, C. W., Liu, X., Chattoraj, J., and Yang, F. (2023). Detecting plant tropism from lidar data. In Chen, T.-W., Kahlen, A. F. K., and Stützel, H., editors, *Book of Abstracts of the 10th International Conference on Functional-Structural Plant Models (FSPM2023)*, pages 123–124.
- Sievänen, R., Godin, C., Dejong, T., and Nikinmaa, E. (2014). Functional-structural plant models: A growing paradigm for plant studies. *Annals of botany*, 114:599–603.
- Soon, K. H. and Khoo, V. H. S. (2017). CITYGML MODELLING FOR SINGAPORE 3D NATIONAL MAPPING. In *ISPRS - International Archives of the Photogrammetry, Remote Sensing and Spatial Information Sciences*, volume XLII-4-W7, pages 37–42. Copernicus GmbH.
- Stava, O., Pirk, S., Kratt, J., Chen, B., Mzch, R., Deussen, O., and Benes, B. (2014). Inverse procedural modelling of trees. *Comput. Graph. Forum*, 33(6):118–131.
- Talle, J. and Kosinka, J. (2020). Evolving l-systems in a competitive environment. In Magnenat-Thalmann, N., Stephanidis, C., Wu, E., Thalmann, D., Sheng, B., Kim, J., Papagiannakis, G., and Gavrilo, M., editors, *Advances in Computer Graphics*, pages 326–350, Cham. Springer International Publishing.
- Vos, J., Evers, J. B., Buck-Sorlin, G. H., Andrieu, B., Chelle, M., and de Visser, P. H. B. (2010). Functional-structural plant modelling: a new versatile tool in crop science. *Journal of Experimental Botany*, 61(8):2101–2115.
- Yi, L., Li, H., Guo, J., Deussen, O., and Zhang, X. (2018). Tree growth modelling constrained by growth equations. *Computer Graphics Forum*, 37(1):239–253.